Real-Coded Genetic Algorithm with Differential Evolution Operator for Terahertz Quasi-Optical Power Divider/Combiner Design

Fan Zhang, Kaijun Song, and Yong Fan

EHF Key Laboratory of Science, School of Electronic Engineering
University of Electronic Science and Technology of China, Chengdu, Sichuan, 611731, P. R. China
ksong@uestc.edu.cn

Abstract ─ This paper describes a modified real-coded genetic algorithm with a differential evolution operator (RGA-DE) for a shaped reflector of terahertz (THz) quasi-optical power divider/combiner. The real-coded genetic algorithm (RGA) is more convenient to define the reflector surfaces as compared to other coding methods. Interpolation method is applied to smooth the sophisticated surfaces. A better searching ability is obtained in a small number of individuals by using the differential evolution operator instead of the conventional crossover operator. So a bionics algorithm combining real-coded genetic algorithm and differential evolution (DE) algorithm has been presented to design the THz quasi-optical multiple-way holographic power-combining circuits. The RGA-DE has been utilized to optimize the coupling coefficient κ of the field distribution to get close to 1. Two real-world examples operating at 380 GHz and 450 GHz respectively are described. The computed results are verified by using the commercial software FEKO Suite.

Index Terms ─Differential evolution operator, quasi-optical power divider/combiner, real-coded genetic algorithm, terahertz technology.

I. INTRODUCTION

Shape optimization is one of the key techniques in the design of a quasi-optical power-combining circuit, which entails optimizing the shape of the metallic reflector [1-5]. The design of large shaped reflector for quasi-optical power-combining circuits has remained a challenge. The shape of the reflector surface is adjusted via a synthesis technique until the pre-defined field distribution is achieved within some acceptable level of accuracy. Numerous synthesis methods based on principles of geometrical optics (GO) [1-2] or physical optics (PO) [3-5] have been developed to compute the electromagnetic wave propagation. In order to get the desired field distribution, the Broyden–Fletcher–Goldfarb–Shanno (LBFGS) algorithm was applied in the past research. But as a gradient optimizer, to get the variation of the target function is a very complicated process. Even if gradient information of a practical problem is available, it can be unreliable or difficult to compute. Thus, non-gradient methods are incredibly useful optimization tools [6].

In this paper, we developed a bionics algorithm combining the real-coded genetic algorithm with a differential evolution operator (RGA-DE) to solve the problem of shaping the reflector surface without gradient information. The conventional genetic algorithm (GA) based on swarm intelligence is easy to be realized and already applied to many fields [7-8]. GA based on real-coding (RGA) can improve the precision of the optimization and the convergence rate [9-10]. But the traditional RGA don't perform well in a small number of individuals and they makes it fall into a local optimum due to the population losing its genetic diversity. Therefore, a differential evolution operator, which is borrowed from the differential evolution algorithm (DE) [11-13], is introduced to, instead of the crossover operator, obtain better searching ability in a small number of individuals.

The remainder of this paper is organized as follows. In Section 2, we introduce the design of the THz quasi-optical power-combining circuits. Subsequently in Section 3, we present RGA-DE to optimize the shape of the metallic reflector. The results achieved, discussed in Section 4, include the verified data by using the commercial software FEKO Suite. Finally, the findings of this paper are summarized in the conclusion.

II. ANALYSIS OF THZ QUASI-OPTICAL POWER-COMBINING CIRCUITS

Power-combining circuits in planar or waveguide structure are more suitable at microwave frequency due to large substrate, ohmic and radiation losses at millimeter- and submillimeter-wave frequencies [14-16]. Therefore, several quasi-optical and spatial holographic power combining techniques performed in free space to avoid these losses attract more and more attention [1-5]. There are two common quasi-optical circuit topology models indicated in Fig. 1. Pyramidal horn antenna and reflector are included in both topology models. But the

Submitted On: July 8, 2017
Accepted On: August 31, 2017

receiving efficiency of such a setup will be strongly decreased if there is mismatch of radiation pattern between the transmitting and receiving radiation patterns. The popular method to solve this problem is to use holography. Figure 1 (a) shows the periodic hologram with a simple stepped surface profile and one shaped reflector. In the other topology, the two shaped reflectors are regarded as computer-generated phase holograms. Both of them are used to shape the electromagnetic wavefront for the field matching.

The surfaces of interest are labeled with P_i, i = 1, 2, 3, 4 in Fig. 1. $\boldsymbol{H}_i$ denotes the field distribution on the surface P_i. The reflectors were assigned parabolic surface to focus the power into the receiving plane P_4 on the antenna array placement. The field on surface P_2 and P_3 in Fig. 1 (a) and on surface P_2 in Fig. 1 (b) can be computed by using the Huygens-Fresnel principle [4]:

$$\boldsymbol{H}_{i+1}(\boldsymbol{r}) = \frac{j}{\lambda_0}\int_{P_i} \boldsymbol{H}_i(\boldsymbol{r}')\frac{e^{-jk_0|\boldsymbol{r}-\boldsymbol{r}'|}}{|\boldsymbol{r}-\boldsymbol{r}'|}\cos(\hat{\boldsymbol{n}}_0, \boldsymbol{r}-\boldsymbol{r}')dp', \quad (1)$$

where $\hat{\boldsymbol{n}}_0$ is the aperture surface's unit normal vector, k_0 is the free space wave number, and λ_0 is the free space wavelength. The computation of the diffraction of each reflector is based on the PO [4, 17]. In the PO for a perfect electric conductor surface, the observation point at r can be computed as:

$$\boldsymbol{H}_{i+1}(\boldsymbol{r}) = \int_{P_i} \boldsymbol{h}(\boldsymbol{r},\boldsymbol{r}')\frac{e^{-jk_0|\boldsymbol{r}-\boldsymbol{r}'|}}{|\boldsymbol{r}-\boldsymbol{r}'|}dp', \quad (2)$$

where

$$\boldsymbol{h}(\boldsymbol{r},\boldsymbol{r}') = -\frac{jk}{2\pi}\hat{\boldsymbol{r}}'\times(\hat{\boldsymbol{n}}'\times\boldsymbol{H}_i(\boldsymbol{r}'))\left(1+\frac{1}{jk_0|\boldsymbol{r}-\boldsymbol{r}'|}\right), \quad (3)$$

where $\hat{\boldsymbol{r}}' = (\boldsymbol{r}-\boldsymbol{r}')/|\boldsymbol{r}-\boldsymbol{r}'|$, $\boldsymbol{H}(\boldsymbol{r}')$ and $\hat{\boldsymbol{n}}'$ denote the magnetic field and the unit normal vector at the integration point $\boldsymbol{r}'$, respectively. When $|\boldsymbol{r}-\boldsymbol{r}'| >> \lambda$, the formula can be written as:

$$\boldsymbol{h}(\boldsymbol{r},\boldsymbol{r}') \approx -\frac{jk}{2\pi}\hat{\boldsymbol{r}}'\times(\hat{\boldsymbol{n}}'\times\boldsymbol{H}_i(\boldsymbol{r}')). \quad (4)$$

In Fig. 1 (b), $\boldsymbol{H}_3$ is calculated by $\boldsymbol{H}_2$ based on PO approximation, and in the same way, $\boldsymbol{H}_4$ in the receiving plane can be obtained by $\boldsymbol{H}_3$. Due to the large electrical dimensions of the reflectors, the computation time is dominated by the integration time. To speed up the computation of the integral, the fast far-field approximation method (FAFFA) is used [18]. In the FAFFA, if $r_{l'l} >> r_{jl'}$ and $r_{l'l} >> r_{li}$, then we have:

$$\frac{e^{-jk_0|\boldsymbol{r}_i-\boldsymbol{r}_j|}}{|\boldsymbol{r}_i-\boldsymbol{r}_j|} \approx \frac{e^{-jk_0(r_{l'l}+\hat{\boldsymbol{r}}_{l'l}\cdot\boldsymbol{r}_{li}+\hat{\boldsymbol{r}}_{l'l}\cdot\boldsymbol{r}_{jl'})}}{r_{l'l}}. \quad (5)$$

Substituting Equation (5) into integral Equations (1) and (2), after three steps of aggregation, translation and disaggregation, the operation count will be reduced from N^2 to $N^{1.5}$. Although the reflector which is one of the most important parts of the quasi-optical power-combining circuit is used to focus the energy on the receiving plane P_4, one reflector with periodic hologram or two simple reflectors cannot get a desired field distribution. Only a small amount of energy in plane P_4 is fed into the receiving antenna array because of the field mismatching. Therefore, a reflector with shaped surface relief is an inevitable choice to get an ideal field distribution.

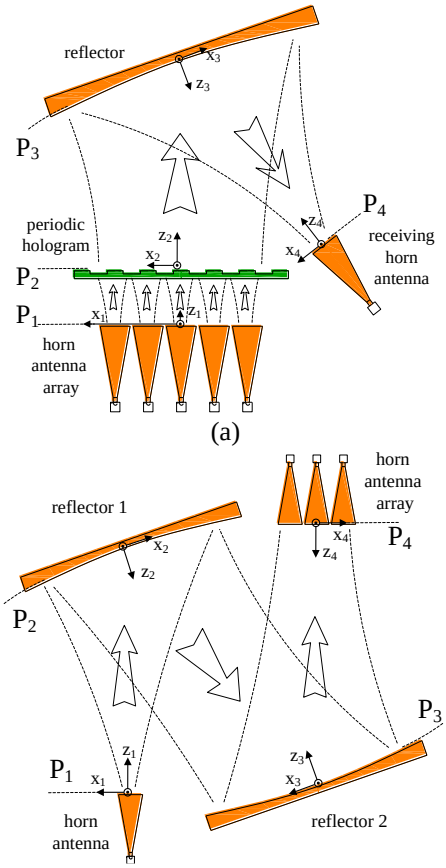

Fig. 1. (a) Power combiner with linear oscillator array, and (b) 2-D quasi-optical power divider consisting of two shaped reflectors.

III. SHAPE OPTIMIZATION VIA RGA-DE

The RGA-DE combines the real genetic algorithm and differential evolution so that a smooth convergence to a more global minimum can be achieved in a small number of individuals. It is noted that the conventional GA may converge slow and to a local minimum. The RGA-DE tends to avoid the aforementioned problem, and is thus, particularly useful for the shaped reflector design.

We first give a detailed coding method for the algorithm. The initial shape of the reflector is parabolic

and this parabolic surface can be expressed in the form:

$$z = \frac{1}{2}\left(\frac{x^2}{R_1} + \frac{y^2}{R_2}\right), \tag{6}$$

where x and y are along the local principal surface directions with R_1 and R_2 being their associated principal surface radii of curvatures.

We discretized the reflector surface into small squares with same periods along the x and y coordinates. The z coordinate of all nodes of the surface can be expressed as a matrix:

$$Z_{parab} = \begin{bmatrix} z_{11} & z_{12} & \cdots & z_{1n} \\ z_{21} & z_{22} & \cdots & z_{2n} \\ \vdots & \vdots & \ddots & \vdots \\ z_{m1} & z_{m2} & \cdots & z_{mn} \end{bmatrix}. \tag{7}$$

In general, $\lambda/3$ gird's width is sufficiently accurate in a practical case. But each grid is variable, meaning, the surface is not smooth after the optimization is completed. Smooth procedures such as low-pass filtering [4] or moving average procedure [5] should be used. Here, an interpolation method is applied to smooth the reflector surface in the real coding.

A certain amount of nodes that are as the optimal variables is enough to interpolate all rest points. *Linear*, *spline* and *cubic* are several common interpolation methods in MATLAB. Interpolation method is a simple and efficient way to yield a smooth surface reflector. The surface correction ΔZ_{interp} interpolates from all interpolating nodes ΔZ. The number of ΔZ_{interp} is about 64 times the number of ΔZ in the following examples. The actual surface relief is:

$$Z_{shaped} = Z_{parab} + \Delta Z_{interp}. \tag{8}$$

The Z_{shaped} will be used in the field calculation. Individuals ΔZ using real-coding can be expressed as below:

$$Z^i(t) = \begin{bmatrix} z_{11}^{ti} & z_{12}^{ti} & \cdots & z_{1q}^{ti} \\ z_{21}^{ti} & z_{22}^{ti} & \cdots & z_{2q}^{ti} \\ \vdots & \vdots & \ddots & \vdots \\ z_{p1}^{ti} & z_{p2}^{ti} & \cdots & z_{pq}^{ti} \end{bmatrix}, \tag{9}$$

where $z_{uv}^{ti} \in [z_{\max}, z_{\min}]$, $u \in [1, p]$, $v \in [1, q]$, $i \in [1, NP]$. NP is the number of individuals in a population. i and t donate the ith individual and the tth generation, respectively. z_{uv}^{ti} which is the interpolation node is as one of the variables pq on the optimization and it is a real number. The variation range of the interpolation node z_{uv}^{ti} is from $z_{\min}$ to $z_{\max}$.

The process of RGA-DE can be represented by the flowchart form as shown in Fig. 2. The loop runs for a number for predefined generations and is composed mainly of evaluate fitness, selection, differential evolution and, mutation steps.

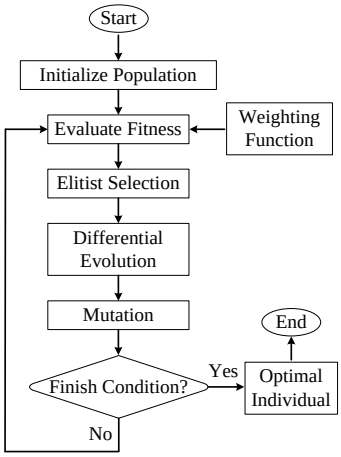

Fig. 2. Flow chart of the proposed RGA-DE.

A. Selection

A selection operator picks individuals based on their fitness function values from a current population and then reproduces these individuals into a differential evolution pool. The individuals that take part in the reproduction step are determined using the roulette wheel method. It means that the individuals are assigned a probability of being selected based on their fitness.

After evolution differential and mutation the new population is generated based on their fitness. With the help of elitism we can store the best found individual. The remaining individual is delivered for the next generation. In this way we cannot lose the best genetics.

B. Differential evolution

Differential evolution operator is to produce new offspring while exploring the solution space. For each individual $Z^i(t)$, a perturbed individual $Z^i(t+1)$ is generated according to scheme DE/best/1 [11], the DE operator is expressed as below:

$$Z^i(t+1) = Z^{best}(t) + F_{DE} \cdot (Z^j(t) - Z^k(t)), \tag{10}$$

with $i, j, k \in [1, NP]$ integer. j and k are picked randomly from 1 to NP for each individual $Z^i(t+1)$, and F_{DE} is a real constant factor, $F_{DE} \in [0, 2]$.

The best performing individual of the current generation $Z^{best}(t)$ will be the perturbed by the differential variation $Z^j(t) - Z^k(t)$, whose amplification is controlled by the constant factor F_{DE}. The DE operator has the advantage of strong local search capability, which is shown in Fig. 3. It is logical to assume that the solution may lie near the parent that has a better fitness.

For a practical problem, if $z_{uv}^{(t+1)i} > z_{\max}$, then let $z_{uv}^{(t+1)i} = z_{\max}$, or if $z_{uv}^{(t+1)i} < z_{\min}$, then let $z_{uv}^{(t+1)i} = z_{\min}$.

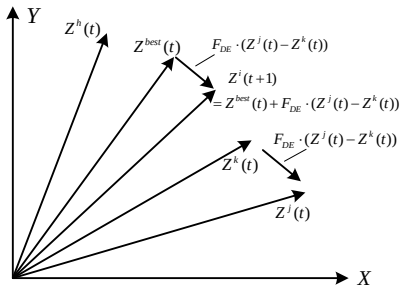

Fig. 3. The process for generating next generation in scheme DE/best/1 showing strong local search capability.

C. Mutation

In DE algorithm, crossover operator is implied to increase the diversity of individuals, but in GA it is realized by mutation. Here, we used a random variation to exploit the solution space.

for n=1 to Q (Mutation number)

Rondomly generate index $u \in [1, p]$ and $v \in [1, q]$.

$z_{uv}^{(t+1)i} = z_{uv}^{ti} + F_m \cdot (z_{random} - z_{uv}^{ti})$;

if $z_{uv}^{(t+1)i} < z_{\min} \,||\, z_{uv}^{(t+1)i} > z_{\max}$

$z_{uv}^{(t+1)i} = z_{\min} + r \cdot (z_{\max} - z_{\min})$;

end

end

where Q is the mutation number, $z_{random} \in [z_{\max}, z_{\min}]$ and r is generated from the interval [0, 1]. The best performing individual in the (t+1)th will not involve in the mutation and it will be preserved in the next generation in the selection operator.

D. Fitness

To quantify the performance of the reflector, we usually use coupling coefficient κ to characterize a potential solution as follows [4]:

$$\kappa = \frac{< H_{cal}, H_{ideal} >_P}{\sqrt{< H_{cal}, H_{cal} >_P < H_{ideal}, H_{ideal} >_P}}, \qquad (11)$$

where H_{cal} and H_{ideal} are the calculated field and ideal field, respectively. The scalar products for two complex-valued vector functions f and g are defined as:

$$< f, g >_P = \int_P f^*(y) g(y) dP(y). \qquad (12)$$

The fitness function of the problem is defined as:

$$fitness = \mathrm{Re}\{\kappa\}. \qquad (13)$$

Sometimes, a weighting function can be applied to guide the evolution in some ways in (11). Using $\tilde{H}_{cal} = H_{cal}.*W_1$ and $\tilde{H}_{ideal} = H_{ideal}.*W_2$ instead of H_{cal} and H_{ideal}, respectively. '.*' denotes element-by-element multiplication. The element of the weighting matrices W_1 and W_2 is usually chosen $\in [0.7, 1.4]$:

$$\tilde{\kappa} = \frac{< \tilde{H}_{cal}, \tilde{H}_{ideal} >_P}{\sqrt{< \tilde{H}_{cal}, \tilde{H}_{cal} >_P < \tilde{H}_{ideal}, \tilde{H}_{ideal} >_P}}. \qquad (14)$$

In the loop runs, $fitness = \mathrm{Re}\{\tilde{\kappa}\}$ can be a candidate to characterize the solution. But when the loop is finished, κ is used to quantify the optimal solution.

IV. NUMERICAL VALIDATION AND DISCUSSION

In order to demonstrate RGA-DE's applicability to real-world problems, two THz quasi-optical holographic power-combining circuits have been designed with RGA-DE. The two circuits are both designed and optimized by MATLAB programming.

The topology model of the first example operating at 380 GHz is shown in Fig. 1 (a), which is a five-way holographic power combiner. The binary phase grating is as a thin lens introducing a phase delay only, which consists of Teflon. The wavefront radiated by the line source consisting of five horn antennas is transformed by the phase grating and is focused to the receiving horn antenna by the shaped reflector. The reflector has a size of about 69λ×48λ. It is discretized to matrices of size 207×144 corresponding to approximately 3 points per wavelength. The optimization result is that κ is approximately 0.88-*j*0.00 at the observation plane 24λ×24λ after two thousand generations, whereas κ is about 0.68+*j*0.13 for the initial shape of the reflector surfaces. The shaped surface obtained for the power divider is illustrated in Fig. 4. Figures 5 (a) and (b) shows the calculated field distribution in the receiving plane P_4.

The parallel computing for each generation of four individuals consumes 15s using a 3.3 GHz quad-core CPU E3-1230v3. Figure 6 shows the progress of both RGA-DE optimization and conventional RGA as the function of the number of generations with different F_{DE}, F_m and NP. In the conventional RGA, the uniform crossover operator is expressed as below:

$$Z^i(t+1) = \alpha \cdot Z^{best}(t) + (1-\alpha) \cdot Z^i(t), \qquad (15)$$

with a constant factor $\alpha = 0.6$ in this paper. It takes about 6.3 hours to complete a single trail with a number of individuals NP = 4 and a fixed mutation number Q = 2. It is obviously that the RGA-DE has a faster convergence speed. The RGA-DE takes only 900 generations to reach the optimal value while the conventional RGA needs 1500 generations. The convergences of different NP are also displayed. In Fig. 6, the numerical results demonstrate that the RGA-DE runs well with high efficiency and stability. It shows that design method based on RGA-DE reached the almost same goal through different routes.

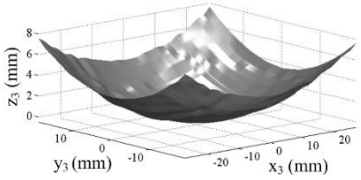

Fig. 4. The surface relief of the reflector.

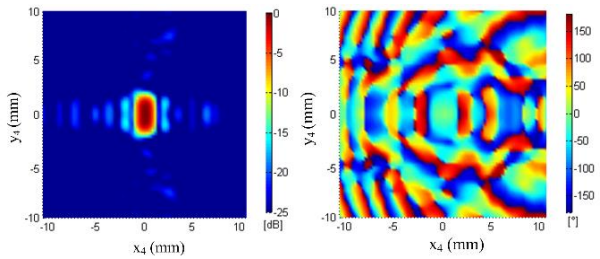

Fig. 5. Optimization results from the presented RGA-DE: (a) magnitude and (b) phase of electric field E_y.

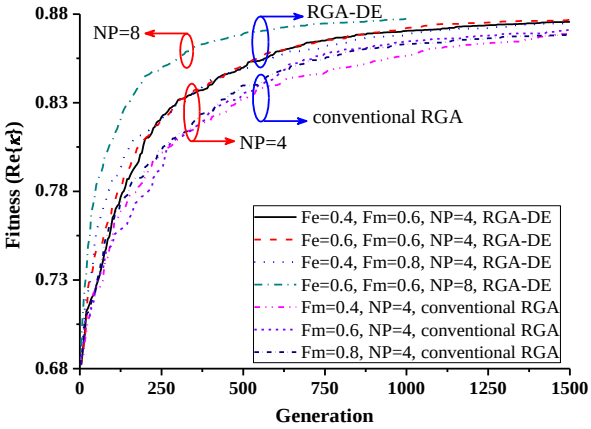

Fig. 6. Convergence characteristics of both RGA-DE and conventional RGA.

The topology model of the second example operating at 450 GHz is shown in Fig. 1 (b), which is a 2-D nine-way (3*3) holographic power combiner. The reflectors both have a size of about 74λ×78λ, which is 42% of the surface area for wavelength scale in [4-5]. The two reflectors are discretized to matrices of size 221×234 corresponding to approximately 3 points per wavelength. The computer-generated holograms, in other words, the shaped surfaces obtained for the power divider are illustrated in Fig. 7.

The optimization result is that κ is approximately 0.89+*j*0.01 at the observation plane 40λ×42λ, whereas κ is about 0.36+*j*0.08 for the initial shape of the reflector surfaces. 64% of the overall radiated power can be received in P_4. Figures 8 (a) and (b) shows the calculated magnetic field distribution in the receiving plane P_4. The correctness of the calculating method and calculated result are verified by using the commercial software FEKO Suite. Figures 8 (c) and (d) shows the verified results. The computation method is MLFMM in FEKO Suite and its calculated field data is imported to MATLAB to draw Figs. 8 (c) and (d). It is noted that the verified results agree closely with the one by PO in MATLAB programming.

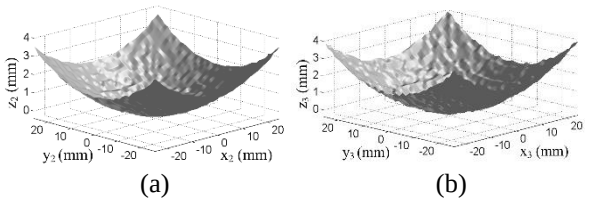

Fig. 7. (a) Surface relief of the first reflector and (b) the second one.

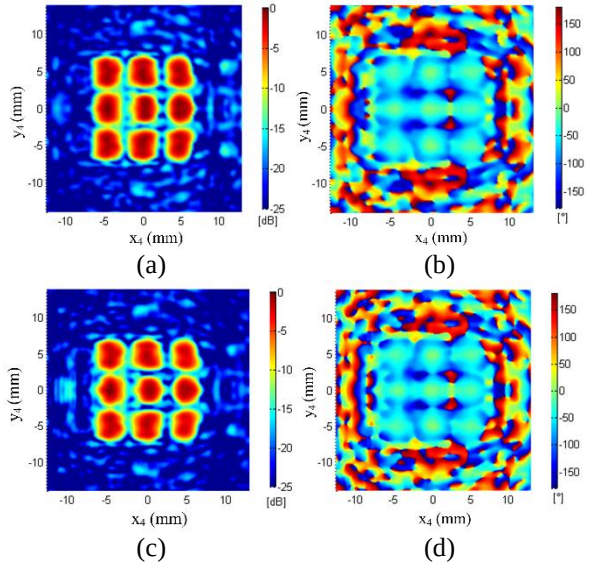

Fig. 8. Optimization results: (a) magnitude, (b) phase of electric field E_y from the presented RGA-DE, (c) magnitude, and (d) phase from the FEKO Suite.

V. CONCLUSION

A bionics algorithm using a differential evolution operator to realize crossover effects in a real-coded genetic algorithm to design the quasi-optical holographic power-combining circuits is investigated at THz frequencies. Real coding with interpolation method is applied to yield a smooth shaped surface. This proposed swarm intelligence optimization algorithm provides a new way to find a solution of complex problems without the gradient information and has good searching ability. It is easy to be realized using parallel computing to improve the computational efficiency. To verify the design and analysis of the THz quasi-optical holographic power-combining circuits, two examples operating at 380 GHz and 450 GHz respectively have been provided. The FEKO Suite's results agree with the optimization ones, which proves that the proposed RGA-DE algorithm is useful in the design of a THz quasi-optical holographic power divider/combiner.

ACKNOWLEDGMENT

The work was supported in part by National Natural Science Foundation of China (Grant No: 61271026) and by the Research Fund of Shanghai Academy of Spaceflight Technology (Grant No: SAST2016094).

REFERENCES

[1] M. Hoft, "Spatial power/combiner in D-band," *IEEE Trans. Microw. Theory Tech*., vol. 52, no. 10, pp. 2379-2384, 2004.

[2] R. Judaschke, M. Hoft, and K. Schunemann, "Quasi-optical 150-GHz power combining oscillator," *IEEE Microw. Wireless Compon. Lett.*, vol. 15, no. 5, pp. 300-302, 2005.

[3] T. Magath, M. Hoft, and R. Judaschke, "A two-dimensional quasi-optical power combining oscillator array with external injection locking," *IEEE Trans. Microw. Theory Tech*., vol. 52, no. 2, pp. 567-572, 2004.

[4] T. Magath, "Diffraction synthesis and experimental verification of a quasi-optical power splitter at 150 GHz," *IEEE Trans. Microw. Theory Tech.*, vol. 52, no. 10, pp. 2385-2389, 2004.

[5] T. Magath, R. Judaschke, and K. Schunemann, "2-D quasi-optical power combining oscillator array at D-band," *Microwave Symposium Diqest, IEEE MTT-S International 2006*, pp. 634-637, 2006.

[6] W. Hare, J. Nutini, and S. Tesfamariam. "A survey of non-gradient optimization methods in structural engineering," *Advances in Engineering Software*, no. 59, pp. 19-28, 2013.

[7] J. H. Holland, *Adaptation in Natural and Artificial Systems: An Introductory Analysis with Applications to Biology, Control, and Artificial Intelligence*. 2nd ed., Cambridge: MIT Press, 1992.

[8] T. Back, U. Hammel, and H. P. Schwefel, "Evolutionary computation: Comments on the history and current state," *IEEE Trans. Evol. Comput.*, vol. 1, no. 1, pp. 3-17, 1997.

[9] K. Chen, X. Yun, Z. He, and C. Han, "Synthesis of sparse planar arrays using modified real genetic algorithm," *IEEE Trans. Antennas and Propagat.*, vol. 55, no. 4, pp. 1067-1073, 2007.

[10] S. R. Rengarajan, "Genetic algorithm optimization of a planar slot array using full wave method-of-moments analysis," *Int. J. Comput. Aid RF Microw. Eng.*, vol. 23, no. 4, pp. 430-436, 2013.

[11] R. Storn, "On the usage of differential evolution for function optimization," *Fuzzy Information Processing Society, NAFIPS, 1996 Biennial Conference of the North American, IEEE*, 1996.

[12] R. Storn, "System design by constraint adaptation and differential evolution," *IEEE Trans. Evol. Comput.*, vol. 3, no. 1, pp. 22-34, 1999.

[13] M. Maddahali, A. Tavakoli, and M. Dehmollaian, "Shape reconstruction of three dimensional conducting objects using opposition-based differential evolution," *Applied Computational Electromagnetics Society Journal*, vol. 32, no. 1, pp. 93-98, Jan. 2017.

[14] K. Song, S. Hu, F. Zhang, and Y. Zhu, "Four-way chained quasi-planar power divider using rectangular coaxial waveguide," *IEEE Microw. Wireless Compon. Lett.*, vol. 25, no. 6, pp. 373-375, 2015.

[15] A. Mahan, S. H. Sedighy, and M. Khalaj-Amirhosseini, "A compact dual-band planar 4-way power divider," *Applied Computational Electromagnetics Society Journal*, vol. 32, no. 3, pp. 243-248, Mar. 2017.

[16] K. Song, F. Zhang, S. Hu, and Y. Fan, "Ku-band 200-W pulsed power amplifier based on waveguide spatially power-combining technique for industrial applications," *IEEE Trans. Ind. Electron.*, vol. 61, no. 8, pp. 4274-4280, 2014.

[17] G. Franceschetti and A. Mohsen, "Recent developments in the analysis of reflector antennas: A review," *IET Microwaves Antennas and Propagation IEE Proceedings H*, vol. 133, no. 1, pp. 65-76, 1986.

[18] C. C. Lu and W. C. Chew, "Fast far-field approximation for calculating the RCS of large objects," *Microwave Opt. Technol. Lett.*, vol. 8, no. 5, pp. 238-241, 1995.

Fan Zhang was born in Hunan, China, in 1989. He received the B.S. degree from the Hefei University of Technology, Hefei, China, in 2012. He is currently working toward the Ph.D. degree in the School of Electronic Engineering, University of Electronic Science and Technology of China, Chengdu, China. He is interested in the investigation of quasi-optical beam-shaping techniques.

Kaijun Song (M'09-SM'12) received the M.S. degree in Radio Physics and the Ph.D. degree in Electromagnetic Field and Microwave Technology from the University of Electronic Science and Technology of China (UESTC), Chengdu, China, in 2005 and 2007, respectively. Since 2007, he has been with the EHF Key Laboratory of Science, School of Electronic Engineering, UESTC, where he is currently a full Professor. He has published more than 80 internationally refereed journal papers. His current research fields include microwave and millimeter-wave/THz power-combining technology;

UWB circuits and technologies; and microwave remote sensing technologies.

Yong Fan received a B.E. degree from Nanjing University of Science and Technology, Nanjing, Jiangsu, China, in 1985, and a M.S. degree from University of Electronic Science and Technology of China, Chengdu, Sichuan, China, in 1992. He is a Senior Member of Chinese Institute of Electronics. From 1985 to 1989, he was interested in microwave integrated circuits. Since 1989, his research interests include millimeter-wave communication, electro-magnetic theory, millimeter-wave technology and millimeter-systems. He has authored or coauthored over 90 papers, 30 of which are searched by SCI and EI.